Mesophyll photosynthetic sensitivity to leaf water potential in *Eucalyptus*: a new dimension of plant adaptation to native moisture supply

Amanda M. Salvi[1] (iD), Duncan D. Smith[1,2,3] (iD), Mark A. Adams[3] (iD), Katherine A. McCulloh[1] (iD) and Thomas J. Givnish[1] (iD)

[1]Department of Botany, University of Wisconsin-Madison, Madison, WI 53705, USA; [2]School of Ecosystem and Forest Sciences, University of Melbourne, Creswick, Vic. 3363, Australia;

[3]Swinburne University of Technology, John Street, Hawthorn, Vic. 3122, Australia

Author for correspondence:
Thomas J. Givnish
Email: givnish@wisc.edu

Summary

- Photosynthetic sensitivity to drought is a fundamental constraint on land-plant evolution and ecosystem function. However, little is known about how the sensitivity of photosynthesis to nonstomal limitations varies among species in the context of phylogenetic relationships.
- Using saplings of 10 *Eucalyptus* species, we measured maximum CO_2-saturated photosynthesis using $A–c_i$ curves at several different leaf water potentials (ψ_{leaf}) to quantify mesophyll photosynthetic sensitivity to ψ_{leaf} (MPS), a measure of how rapidly nonstomal limitations to carbon uptake increase with declining ψ_{leaf}. MPS was compared to the macroclimatic moisture availability of the species' native habitats, while accounting for phylogenetic relationships.
- We found that species native to mesic habitats have greater MPS but higher maximum photosynthetic rates during non-water-stressed conditions, revealing a trade-off between maximum photosynthesis and drought sensitivity. Species with lower turgor loss points have lower MPS, indicating coordination among photosynthetic and water-relations traits.
- By accounting for phylogenetic relationships among closely related species, we provide the first compelling evidence that MPS in *Eucalyptus* evolved in an adaptive fashion with climatically determined moisture availability, opening the way for further study of this poorly explored dimension of plant adaptation to drought.

Introduction

Throughout evolutionary history, terrestrial vascular plants have faced a fundamental trade-off between the photosynthetic assimilation of atmospheric carbon and transpirational loss of water through stomata (Givnish & Vermeij, 1976; Cowan & Farquhar, 1977; Givnish, 1986). When faced with water deficits on a daily, seasonal, or annual basis, plants exhibit declines in photosynthetic rates. Such reduced rates have been viewed as solely reflecting a drop in stomatal conductance (Cowan & Farquhar, 1977; Medlyn *et al.*, 2011). However, there is increasing evidence that water stress – specifically, declines in leaf water potential ψ_{leaf} – also reduces photosynthesis independent of stomatal limitations (Tezara et al., 1999, 2002, 2003; Tang *et al.*, 2002; Lawlor & Tezara, 2009; Zhou *et al.*, 2013, 2014; Dewar *et al.*, 2018; Salmon *et al.*, 2020). The sensitivity of photosynthesis to these nonstomal limitations, which hereafter we refer to as mesophyll photosynthetic sensitivity (MPS), may have been a fundamental constraint on land plant evolution, selecting for the rise and optimization of traits that conserve, transport, or access water, including stomata, vascular systems, and roots

(Givnish, 1986). Recent advances in understanding of these photosynthetic limitations across the entire land plant phylogeny show that angiosperms display a more balanced colimitation of diffusional and biochemical limitations than early diverging plant groups. While this is an intriguing example of the importance of photosynthetic capacity in plant evolution (Gago *et al.*, 2019), we know little about variation in MPS and especially how MPS varies among closely related plants native to different ecological conditions while accounting for phylogenetic similarity.

Evidence of nonstomal limitations of photosynthetic performance is largely derived from measured responses of CO_2 assimilation rates (A) to internal concentrations of CO_2 (c_i). A change in c_i at a given atmospheric $[CO_2]$ is caused by stomatal limitation, while a change in the shape of the A-c_i response is due to nonstomal limitations. Thus, the effects of stomatal conductance can be accounted for (and removed) by comparing A-c_i 'response curves' (Tezara *et al.*, 1999, 2002, 2003; Zhou *et al.*, 2013; Salmon *et al.*, 2020). Declines in maximum apparent rates of CO_2 assimilation (the asymptote of an A-c_i curve) as ψ_{leaf} declines have been interpreted as impaired photosynthetic metabolism and/or mesophyll

conductance of CO_2 to sites of photosynthesis. This interpreted limitation has been the subject of considerable scrutiny. One concern is of possible artifacts when measurements of A and c_i are made at extremely low values of stomatal conductance. Precautions are therefore needed when measuring very small changes in CO_2 concentrations. For example, the diffusional leakage of CO_2 through clamp-on leaf chambers can be taken into account by quantifying the coefficient of CO_2 diffusional leakage of the chamber using thermally killed leaves (Flexas *et al.*, 2007). Additional evidence for non-stomatal limitation is provided by the decline in photosynthesis with leaf water potential in *Helianthus* even after the epidermis has been peeled away, obviating the need for A-c_i curves and a calculation of c_i (Tang *et al.*, 2002). Kelp, which lack stomata and internal air spaces, display similar relationships of photosynthesis and water potential (Kawamitsu *et al.*, 2000). The present state of knowledge is that properties of the mesophyll contribute to overall reductions in photosynthesis at reduced ψ_{leaf}.

Substantial research has been conducted to identify the different types of nonstomatal limitations to photosynthesis and how and to what extent these processes restrict photosynthetic capacity. Water stress, whether caused by short- or long-term drought, salt inundation, or diurnal changes in leaf water potential or vapor pressure deficit, has clear effects on carboxylation capacity, electron transport, mesophyll conductance, chloroplast ATP production, and/or RuBisCO concentration and activity. In each case, apparent photosynthetic capacity within leaves is considerably reduced (Ball & Farquhar, 1984; Tezara *et al.*, 1999; Galmés *et al.*, 2013; Zhou *et al.*, 2013, 2014; Dewar *et al.*, 2018; Flexas *et al.*, 2018; Nadal & Flexas, 2018; Wang *et al.*, 2018). Nevertheless, how these limitations affect apparent mesophyll photosynthetic capacity remains poorly studied, and these limitations may vary considerably among plants of different ecological and phylogenetic histories. Two studies of mesophyll photosynthetic capacity in response to drought suggest that species native to moister environments had greater vulnerability to water stress (Zhou *et al.*, 2013, 2014). However, these studies involve confounding variation in leaf phenology, growth form, and/or N-fixing ability, and lack the statistical analyses required to account for phylogenetic relationships, or draw justified conclusions regarding trait–trait and trait–environment relationships. More comprehensive studies are thus needed to determine the adaptive importance of mesophyll photosynthetic sensitivity and how it varies in different ecological and phylogenetic contexts, in order to better understand plant adaptations to drought, both historically and in the context of current anthropogenic climate change. Attempts have also been made to quantify the fractional limitations of photosynthesis due to stomata vs apparent variation in mesophyll conductance (g_m) and leaf biochemistry (Grassi & Magnani, 2005; Carriquí *et al.*, 2015; Xiong *et al.*, 2018; Gago *et al.*, 2019). However, separating the effects of supposed variation in mesophyll conductance is problematic and often depends on several parameters measured in species other than those under study and untested assumptions.

We sought to quantify the holistic effects of nonstomatal limitations on mesophyll photosynthetic capacity (that is,

photosynthetic rates obtained after removing the effect of stomatal limitations via use of A–c_i curves at different values of ψ_{leaf}, following the approach pioneered by Tezara *et al.*, 1999, but see also Salmon *et al.*, 2020). We measured the sensitivity of A–c_i curves to leaf water potential, in order to understand MPS – the sensitivity of nonstomatal photosynthetic limitations to drought. We quantified mesophyll photosynthetic sensitivity in two ways: ψ_{50}, the leaf water potential at a 50% decline from maximum photosynthetic rates, and β, the maximum slope of decline in photosynthetic rates with declining ψ_{leaf}. Our aim was to understand differential adaptation of MPS to environmental conditions within a set of species that are closely related but differ strikingly in their ecological distributions. Closely related species share a common evolutionary heritage, so that studying physiological differences among them may be less clouded by the greater genetic differences that have accumulated, for a variety of idiosyncratic reasons, among species in distantly related lineages. Studying ecophysiological differences among close relatives in a phylogenetic framework can provide important insights into how individual species diverged and became able to dominate different portions of environmental gradients. Such an approach – including phylogenetic relationships explicitly in all statistical analyses – permits rigorous tests of the roles of ecology vs phylogeny in determining plant traits and their adaptation to environmental conditions (e.g. see Givnish & Montgomery, 2014).

Here we predict that species native to drier climates should exhibit lower mesophyll photosynthetic sensitivity – defined by more negative ψ_{50} and larger β – and that MPS should be correlated with other adaptations to drought (e.g. more negative turgor loss points, Bartlett, Scoffoni & Sack, 2012; Fu & Meinzer, 2018). Furthermore, we expect that lower MPS, as an adaptation to drought, should be accompanied by reduced rates of maximum leaf-level photosynthesis at full hydration, in accordance with the theoretically expected and empirically observed trade-off of maximum photosynthetic rate and drought sensitivity (Givnish & Vermeij, 1976; Orians & Solbrig, 1977; Temme *et al.*, 2019).

We used glasshouse and common-garden experiments to provide the first phylogenetically comparative data on mesophyll photosynthetic sensitivity across a large set of ecologically divergent but closely related species in the genus *Eucalyptus*. *Eucalyptus* is a powerful model system given the differential distribution of its species along extensive moisture gradients (Schulze *et al.*, 1998, 2006; Miller *et al.*, 2001; Nicolle, 2006; Atlas of Living Australia: http://www.ala.org.au), their radiation during times of aridification (Crisp *et al.*, 2004; Bui *et al.*, 2017; Thornhill *et al.*, 2019), diversity in physiological traits (Schulze *et al.*, 1998, 2006; Warren & Adams, 2005; Warren *et al.*, 2006; Turner *et al.*, 2008; Cernusak *et al.*, 2011; Givnish *et al.*, 2014), and the existence of a DNA phylogeny required for the rigorous comparative analyses needed to interpret the roles of ecology vs phylogeny in shaping the characteristics and distributions of extant species (Li *et al.*, 2018; Thornhill *et al.*, 2019).

Materials and Methods

Study system

We investigated differences in mesophyll photosynthetic sensitivity (MPS) across ten species of *Eucalyptus*. The species – *Eucalyptus dumosa* A. Cunn. ex J. Oxley, *Eucalyptus microcarpa* (Maiden) Maiden, *Eucalyptus sideroxylon* A. Cunn. ex Woolls, *Eucalyptus viminalis* Labill, and *Eucalyptus nitens* (H. Deane & Maiden) Maiden *of subgenus Symphyomyrtus*, and *Eucalyptus arenacea* Marginson & P. Ladiges, *Eucalyptus macrorhyncha* F. Muell. ex Benth, *Eucalyptus dives* Schauer, *Eucalyptus obliqua* L'Hér, and *Eucalyptus regnans* F. Muell of subgenus *Eucalyptus* (see Supporting Information Fig. S1 for phylogenetic tree) – were stratified by phylogeny and by dominance of different portions of a macroclimatic gradient, as measured by P/E_p (the ratio of annual precipitation to pan evaporation) in south eastern Australia. Our ten study species have a mean annual rainfall (P) ranging from 350 mm to 1043 mm, with mean P/E_p varying fivefold, from 0.19 to 0.98 (Fig. 1; Table S1); these species range from cool temperate rain forest and tall wet sclerophyll forest, to open forest, woodland, and mallee (an Australian arid to semi-arid habitat named for the multi-stemmed eucalypt growth forms that are common there; mallet eucalypts have single small stems emerging from a lignotuber).

Species occurrences and climate data

Species occurrences were obtained from the Atlas of Living Australia (ALA) database on 19 May 2018. To avoid effects of over-sampling, latitude and longitude were rounded to the nearest 0.25 degree and duplicate species–location combinations were removed. We inspected spatial distributions and removed clear visual outliers ($n = 3$ points; likely from a botanic garden or incorrectly identified). For each location, we extracted climate variables (mean annual precipitation (P) and temperature) from WorldClim (Fick & Hijmans, 2017) using QGIS 3.0 (QGIS Development Team, 2018). Pan evaporation (E_p) was extracted for each location from the Bureau of Meterology's (BOM) 0.25-degree resolution dataset (http://www.bom.gov.au/jsp/ncc/climate_averages/evaporation/index.jsp?period=anu#maps) using R v.3.6.2 (R Core Team, 2019). We calculated P/E_p of each occurrence and then took the mean for each species.

Plant material and glasshouse growing conditions

Seeds were obtained from Forest Seeds Australia (Bacchus Marsh, Victoria), Goulburn Broken Indigenous Seedbank (Dookie, Victoria), and Commonwealth Scientific and Industrial Research Organisation (CSIRO) Australian Tree Seed Centre (Black Mountain, Australian Capital Territory). Precise provenances for those seeds are not known for most species. A key assumption of multi-species studies like the one presented here is that the signal of trait or performance differences across a wide set of species that occupy different parts of an extensive ecological gradient will overwhelm the effects of exactly where along that gradient material of a given species was chosen for study.

In early 2018, plants were germinated in flat beds of field soil and transplanted to 10-cm tall pots filled with Pro-mix BX potting medium (Premier Tech Horticulture, Riviere-du-Loup, Québec, Canada) at a glasshouse at the University of Wisconsin–Madison. Once a substantial rooting system had developed and saplings were about 5 cm tall, saplings were moved to 35-cm tall plastic pots filled with equal parts sand : field soil : Promix® BX, and fertilized once to twice per week. Plants were hand-watered to maintain a nonlimiting water supply during this initial growth. Espoma Organic Soil Acidifier was added periodically to maintain neutral pH, as irrigation water was somewhat calcareous. Experiments were conducted from May to October 2018. While heteroblasty is common across the genus *Eucalyptus*, most of our species show relatively little heteroblasty, with *E. nitens*, *E. arenacea* and *E. dives* being exceptions. Juvenile foliage was still present in *E. nitens*, *E. dives*, *E. viminalis* and *E. arenacea* during measurements. All measurements were conducted at the same age post germination. Air temperature was regulated, ranging from 25–30°C during the day to 14–20°C at night. Artificial overhead lighting was added if environmental PPFD fell below 600 μmol m^{-2} s^{-1}. Locations of plants in the glasshouse were randomized biweekly to minimize effects of differences in conditions across the glasshouse.

Gas exchange and leaf water potential measurements

We withheld water from eight to 11 plants per species over 1–2 wk and measured their mesophyll photosynthetic capacity across several days during this slow dry-down. Net CO_2 exchange (A) and stomatal conductance (g_s) was measured on the youngest fully expanded leaves at light saturation (1500 μmol m^{-2} s^{-1}; 10% blue light) and 28°C block temperature with a portable photosynthetic gas exchange system (LI-6400XT; Li-Cor Inc., Lincoln, NE, USA). Leaf vapor pressure deficit (VPD) was maintained as close as possible to 2 kPa during all measurements using desiccant within the LI6400 system, with a standard deviation of 0.4. Cuvette reference CO_2 concentration (atmospheric CO_2 concentration, c_a) during measurements was varied as follows: 400, 200, 100, 50, 800, 1600 and 2000 μmol CO_2 mol^{-1} air. Effects of stomatal control were largely accounted for by comparing A to leaf internal CO_2 concentration (c_i), which is a calculation accounting for the ability of CO_2 to diffuse into the leaf. Thus, we interpret stomatal limitation as a change in c_i and nonstomatal limitation as a change in the $A–c_i$ curve. Before starting these measurements, we acclimated the leaf in the cuvette for 10–20 min at 400 μmol CO_2 mol^{-1} air to achieve stable gas exchange, and then allowed gas exchange to equilibrate for 3–5 min at each CO_2 step before logging data. We corrected for diffusion leakage of CO_2 through the infrared gas analyzer's leaf gaskets (IRGA)'s by additionally conducting $A–c_i$ curves on boiled (i.e. photosynthetically inactive) leaves (see Flexas *et al.*, 2007). Actual A values from experimental $A–c_i$ curves were corrected by subtracting the relationship between c_a and the 'apparent' photosynthesis of an inactivated leaf. The resulting $A–c_i$
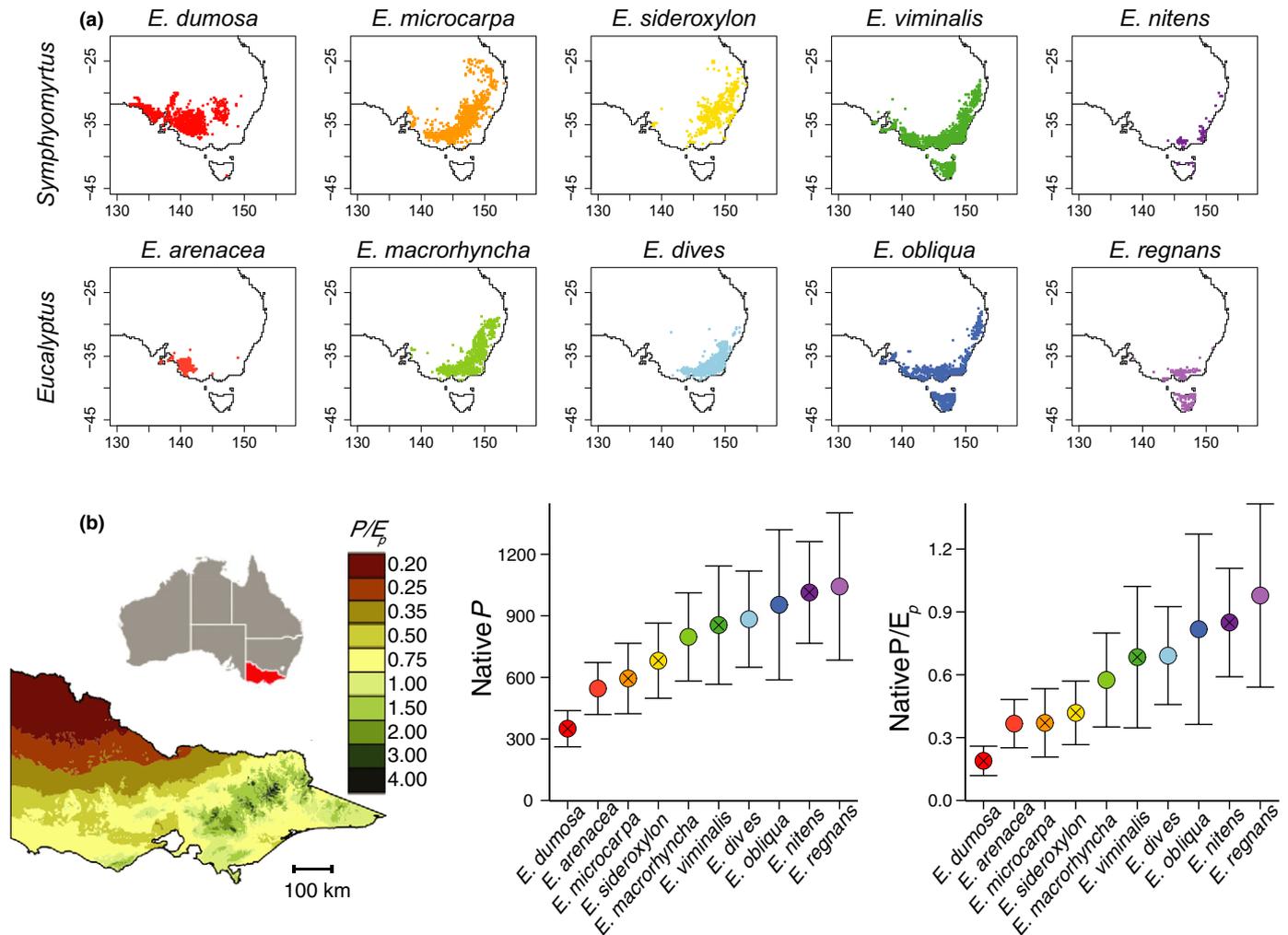
Fig. 1 Native distributions and climate data for the 10 *Eucalyptus* species. (a) Geographic distributions (latitude × longitude) across Australia, ranked by subgenus (rows) and moisture supply (least on the left). (b) Map of Victoria, reproduced from Givnish *et al*. (2014), showing contours of the moisture gradient – the ratio of annual precipitation to annual pan evaporation (P/E_p). (c) Mean annual precipitation (P). (d) Native mean P/E_p. Error bars represent one SD. Crossed circles indicate subgenus *Symphyomyrtus*.

curves provide measures of mesophyll photosynthetic capacity, also known as apparent photosynthetic capacity (Zhou *et al.*, 2013), with the effect of stomatal conductance accounted for and technical artifacts largely subtracted. However, mesophyll conductance was not quantified, and our measured mesophyll photosynthetic capacity is still limited by a combination of CO_2 diffusivity through cells and biochemical effects. After completion of each $A–c_i$ curve, the leaf was excised and leaf water potential (ψ_{leaf}) was measured using a Scholander-type pressure chamber (PMS Instruments, Albany, OR, USA) after allowing for equilibration (about 5–10 min). To minimize temporal bias during data collection, we droughted plants in batches, using one plant per species until the last individual died of drought stress, before beginning a new drought experiment for all species. After several dry downs, some large gaps in leaf water potential remained, particularly at lower ψ_{leaf}. To fill gaps during later iterations of dry downs, we often measured individuals only when they were at ψ_{leaf} values that fell within gaps. In this way, some

individuals have several repeated measurements (33% with four or more repeated measurements), some have few (44% with two to three), and others have no repeated measurements (22% with one measurement).

Quantifying mesophyll photosynthetic sensitivity

Each $A–c_i$ curve was analyzed using the Farquhar–Berry–von Caemmerer model of photosynthesis (Farquhar *et al.*, 1980) using R package PLANTECOPHYS (Duursma, 2015) with the assumption that mesophyll conductance was infinite. In this way, any change in $A–c_i$ curves with water potential could be due to changes in g_m and/or biochemical limitations. While $A–c_i$ curves are conventionally parameterized with maximum carboxylation and electron transport rates (V_{cmax} and J_{max}, respectively), we instead quantified the maximum rate of gross photosynthesis (A_{max}) for each $A–c_i$ curve. This approach implicitly includes the effects of g_m in a way that compensates to a great extent for its

explicit exclusion (Knauer *et al.*, 2020). In this paper, we present results based on the parameterization of A_{max}, which was calculated as R_d (estimated from the A–c_i photosynthetic model) plus the A predicted from the A–c_i model at maximum $c_i = 6000\ \mu mol\ mol^{-1}$. Values of A_{max} per unit area were converted to a mass basis using the species' mean specific leaf area (SLA); mass-based rates can be more important determinants of whole-plant rates of growth than area-based rates, given that they measure energetic returns per unit investment (see Givnish, 1988; Kruger & Volin, 2006). Specific leaf area data were obtained from one young, fully expanded leaf (excluding petioles) from six plants per species. Leaves were scanned with a leaf area scanning conveyer belt (LI-3100C; Li-Cor Inc.), and then dried at 70°C for 1 d and weighed. Raw data for A_{max} and sensitivity to ψ_{leaf} are presented in Fig. S2. For reference, apparent values of V_{cmax} and J_{max} are presented and analyzed for sensitivity to ψ_{leaf} in Figs S5–S7.

Analytical model for mesophyll photosynthetic sensitivity

A sigmoidal response curve of A_{max} to ψ_{leaf} was fit for the data of each species using R function 'SSlogis' (R Core Team, 2019):

$$A_{max} = M/(1 + \exp[\beta(y_{50} - y_{leaf})])\qquad \text{Eqn 1}$$

where M is the value of A_{max} under moist conditions ($\psi_{leaf} = 0$; effectively the maximum theoretical A_{max}), β is a slope coefficient indicating the steepness of the decline, and ψ_{50} is the ψ_{leaf} at which A_{max} decreases to half M. See the Results section and Figs. S2,S3 for information on how and why this equation was fit to data. Random effects by individual plants were not incorporated due to the sizeable number of individuals that were not repeatedly measured.

Measuring turgor loss point

Turgor loss points (TLP, units MPa), the ψ_{leaf} at turgor loss, were calculated for five leaves or small leafy shoots of each species from pressure–volume curves generated using the bench dry method (Tyree & Hammel, 1972). Briefly, leaves were cut from the branch at the petiole in the early morning before transpiration had reached a maximum, and placed in water and out of direct sunlight to hydrate for 20–30 min. We measured ψ_{leaf} using a Scholander-type pressure chamber (PMS Instruments) and then leaf mass; this was repeated 8–19 times until a plot of $-1/\psi_{leaf}$ vs leaf mass lost formed a linear region, where it is assumed that turgor pressure equals zero. The equation of this linear region can be used to calculate pressure (ψ_P) and osmotic potentials ($\psi\pi$) at any given ψ_{leaf}. Turgor loss point is ψ_{leaf} when $\psi_P = 0$. Photosynthetic safety margin was calculated as the difference (in MPa) between TLP and ψ_{50} A_{max}.

Photosynthetic rates in common gardens

Using the methods described earlier, we conducted A–c_i curves for the same 10 *Eucalyptus* species at four common gardens across

Victoria, Australia (see Table S2 for geographic coordinates and climatic and soil information) between October 2018 and February 2019. As we were interested in estimating the maximum A_{max} per species per site, we generally used the largest five A_{max} values per species per site taken when $\psi_{leaf} > -1.5$ MPa, which should precede any declines in A_{max} across species based on our glasshouse experiments. For a few species × site combinations, $n = 2$–4, due to low survival rates or plants drying down very quickly out of the > -1.5 MPa range. Study species were planted at the sites in June 2018 on a 30-cm square grid. A_{max} was converted from a per area basis to a per mass basis, using the species' mean SLA at the site. Most SLA data were obtained in March and April 2019 from one young, fully expanded leaf from generally eight plants per species × site. From each leaf, 16 mm punches were taken, avoiding the mid-vein when possible. When leaf disks were incomplete circles, they were immediately photographed for area determination. Photographs were corrected for lens distortion using PTLens (ePaperPress, Portland, OR, USA) and analyzed in ImageJ (NIH, Bethesda, MD, USA). Four species (*E. dives*, *E. nitens*, *E. obliqua* and *E. regnans*) at the driest site, Hattah, did not survive for these SLA measurements. For all except *E. dives*, we measured SLA using entire lamina from similar-aged plants grown at the site 1 yr prior. For *E. dives*, we collected leaf disks in December 2019 at the second driest site, Bealiba, and used these for both Bealiba and Hattah. All SLA samples were later dried at 70°C and weighed.

Leaf nitrogen content

We tested whether observed reductions in photosynthesis with water stress could be complicated by reductions in leaf nitrogen, which largely reflects leaf RuBisCO content. At the beginning and end of the glasshouse water-deprivation experiments, we excised leaves excluding petioles of five plants (except for *E. obliqua* and *E. macrorhyncha*, which had $n = 4$ and 6, respectively, for post-drought), then oven-dried, ground, and sent them to the Central Appalachians Stable Isotope Facility to measure percent leaf N. Pre-drought samples were collected on the first day of A–c_i measurements, when ψ_{leaf} was at its maximum. Post-drought samples were collected on the individual's last day of A–c_i measurements, when ψ_{leaf} was at its minimum and leaves on the plant were visibly wilted, but the plant was not dead (judged by gas exchange, shedding crisp dried leaves, and twigs breaking off at touch).

Recovery of mesophyll photosynthetic capacity after rehydration

To investigate whether mesophyll photosynthetic capacity can recover after a drought event, we compared A_{max} in plants before drought to those after plants were rehydrated post-drought. Using three selected species that fall at the driest, middle, and wettest parts of the natural macroclimatic moisture gradient within our study system (*E. dumosa*, *Eucalyptus tricarpa* (L.A.S. Johnson) L.A.S. Johnson & K.D. Hill, and *E. regnans*, respectively; *E. tricarpa* is a sister species of *E. sideroxylon*) and five

individuals per species, we measured A–c_i curves and ψ_{leaf} using previously described methods on the first day of drought treatment. Plants were allowed to slowly dry down until most leaves on the plant were visibly wilting, where plants were then watered and maintained at soil field capacity for 2 d, allowing the plants to rehydrate. On this second day of rehydration conditions, when ψ_{leaf} had returned to near pre-drought values, we measured A–c_i curves and ψ_{leaf} values.

Statistical analyses

In addition to ordinary simple linear regressions, we used phylogenetically structured linear regressions (Ho & Ané, 2014) to test for significant relationships of mesophyll photosynthetic sensitivity parameters (β and ψ_{50}) to the position of species along the moisture gradient (mean P/E_p) and species' TLP using Pagel's λ (based on a Brownian motion model) and the R package PHYLOLM (Ho & Ané, 2014). We used the R package PHYTOOLS (Revell, 2012) to obtain relationships and times of divergence among our study species from the time-calibrated molecular phylogeny of Thornhill *et al.,* (2019) (see Fig. S1). Based on Bayesian analysis, 59.2 Ma is the estimated crown age for all eucalypts (*Angophora, Corymbia* and *Eucalyptus*), with estimates of 33.4 Ma for subgenus *Eucalyptus*, and 32.5 Ma for *Symphyomyrtus* (Thornhill *et al.,* 2019). To test for significant differences in slope and intercept between the two subgenera, we conducted ordinary and phylogenetically structured ANCOVAs (Ho & Ané, 2014). We used an analysis of deviance test of linear mixed-effects models to investigate whether drought conditions had an effect on leaf nitrogen content (%N), and to compare mesophyll photosynthetic capacity before drought and after rehydration post-drought. In common garden experiments, we used an ANOVA F-test for model selection (testing for slope and/or intercept differences). Using this selected model, we then used a linear regression to test for a relationship between maximum A_{max} and native P/E_p. We could not investigate phylogenetic effects here, as the R package PHYLOLM is limited for use with data that has only one value per species (Ho & Ané, 2014). See the Discussion section for more on this limitation. All analyses were done using R v.3.6.2 (R Core Team, 2019). Package GGPLOT2 was used for figure making (Wickham, 2016).

Results

In the glasshouse, A_{max} declined nonlinearly with ψ_{leaf} in all species (Figs 2a, S2). A sigmoidal equation provided a better fit of these drought responses than linear or exponential functions, as determined using the Akaike information criterion (AIC values for sigmoidal/exponential/linear responses to ψ_{leaf}: A_{max} are −253/−219/−231. See Fig. S3 for additional details regarding model selection). We found that leaf %N content in pre-drought plants was *c.* 0.17% greater than in the same plants post-drought – a small but significant effect ($P_{df=9} = 0.0001$, mixed model; Fig. S4). There was large variation among species in their quantitative response: ψ_{50} A_{max} ranged from −4.08 to 2.08, and β of the A_{max} sigmoidal response model ranged from 1.2 to 6.69 (Table S2; referred to hereafter as β A_{max}). As we predicted,

drought response was related in a systematic fashion to species' distributions along the macroclimatic moisture gradient. As native P/E_p declined, ψ_{50} of the A_{max} sigmoidal response model (hereafter, ψ_{50} A_{max}) became more negative. The decline in ψ_{50} A_{max} with native P/E_p was significant in both ordinary ($P_{ord} = 0.01$) and phylogenetically structured ($P_{phy} = 0.012$) linear regressions (Fig. 2b). Table 1 provides a summary of linear regression models, and Table S3 provides all statistical results. Phylogenetically structured ANCOVAs of ψ_{50} A_{max} vs native P/E_p revealed that neither slopes nor intercepts differed significantly between subgenera. We also found that the slope coefficients (β) of the sigmoidal function describing A_{max} increased significantly with native P/E_p ($P_{ord} = P_{phy} < 0.02$; Fig. 2c; Table 1), although standard deviations were large. Ordinary and phylogenetically structured linear regressions were identical in these cases, indicating no phylogenetic signal. However, ANCOVAs revealed some evidence within relationships of β A_{max} vs P/E_p that slopes were significantly greater in subgenus *Eucalyptus* ($P = 0.07$ and 0.03, respectively; Table S3) than in subgenus *Symphyomyrtus*. While we do not present this data here, analysis of A–c_i curves also led to J_{max} and V_{cmax} declining as ψ_{leaf} declines, and at lower rates in drier habitats, in a pattern complementary to A_{max}.

Maximum mesophyll photosynthetic capacity at full hydration – as measured by A_{max} at $\psi_{leaf} = 0$ MPa – increased as predicted with native P/E_p within the glasshouse study, but not significantly so ($P_{ord/phy} > 0.10$; Table 1). There was also no significant relationship between maximum mesophyll photosynthetic capacity and ψ_{leaf}. However, we found that A_{max} did increase with native P/E_p, as predicted, in plants grown across four common gardens in the field in Victoria (Fig. 3; $P < 0.001$). The best model allowed for intercept but not slope differences across sites (ANOVA F test: intercept differences $P < 0.001$, slope differences $P = 0.13$).

To determine how MPS may relate to other measures of water stress tolerance, we compared ψ_{50} values to turgor loss point (TLP), the ψ_{leaf} at leaf wilting. Turgor loss point is a well-recognized measure of drought tolerance, where more negative TLP is associated with greater tolerance (Bartlett *et al.,* 2012; Fu & Meinzer, 2018). Across our ten species, TLP ranged from an average ($n = 5$) of −2.3 MPa (*E. dumosa*) to −1.0 MPa (*E. obliqua*), and increased significantly with both native P/E_p ($P_{ord} = 0.03$; $P_{phy} = 0.002$; Fig. 4a) and ψ_{50} A_{max} ($P_{ord} = P_{phy} = 0.002$; Fig. 4b). ψ_{50} A_{max} was more negative than TLP across species, and the difference between TLP and ψ_{50} A_{max} (photosynthetic safety margin) became smaller as P/E_p increased ($P_{ord} = P_{phy} = 0.04$; Fig. 4c).

We found that ψ_{leaf} at maximum drought was significantly more negative than pre-drought and rehydrated groups ($P_{df=4} < 0.001$, mixed model), indicating that plants experienced drought and were then successfully rehydrated to close to initial conditions (Fig. 5b). A_{max} did not differ significantly between pre-drought and rehydrated treatments in any of the three species ($P_{df=2} > 0.1$, mixed model; Fig. 5a). Thus, within the limits of our study, the declines in mesophyll photosynthetic capacity with decreasing leaf water potential were completely reversible. There were no
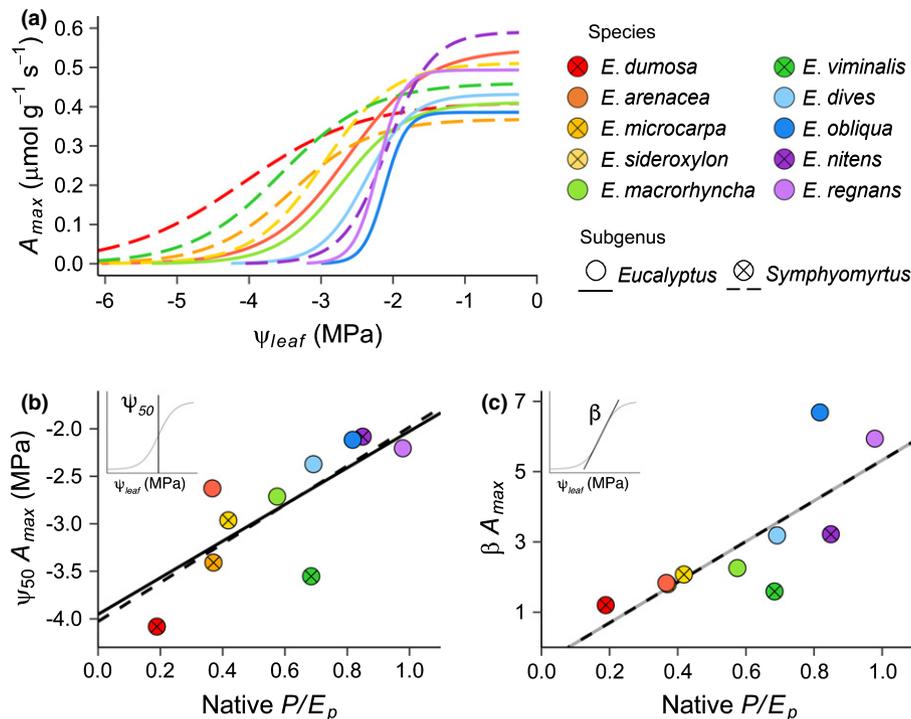
Fig. 2 Mesophyll photosynthetic sensitivity to leaf water potential. (a) Response of gross photosynthesis (A_{max}) to leaf water potential (ψ_{leaf}) in 10 *Eucalyptus* species native to different portions of a steep moisture gradient (measured by the ratio of annual precipitation to annual pan evaporation, P/E_p) in Victoria, Australia. (b) $\psi_{50}A_{max}$ vs native P/E_p. Inset in (b) visualizes $\psi_{50}A_{max}$ (the ψ_{leaf} at a 50% decline from maximum gross photosynthetic rates), on a sigmoidal curve. The solid black line is the phylogenetically structured linear regression, and the dashed black line is ordinary linear regression. (c) βA_{max} vs native P/E_p. Inset in (c) visualizes β (the maximum slope of decline in photosynthetic rates with declining ψ_{leaf}) on a sigmoidal curve. The black and gray dashed line indicates that both phylogenetic and ordinary linear regressions yield the same results. See Supporting Information Table S2 for values and standard errors, and Table S3 for complete summary statistics.

Table 1 Ordinary and phylogenetically structured linear regression models relating measures of mesophyll photosynthetic sensitivity (MPS), turgor loss point (TLP), and photosynthetic safety margin to native moisture availability (P/E_p) for 10 *Eucalyptus* species, and TLP as a function $\psi_{50} A_{max}$.

	Ordinary linear regression	Phylogenetically structured regression
Relationship to P/E_p		
$\psi_{50} A_{max}$	$y = 2.05x - 4.03$**	$y = 1.93x - 3.95$**
βA_{max}	$y = 5.78x - 0.46$***	$y = 5.78x - 0.46$***
A_{max} at $\psi_{leaf} = 0$ MPa	$y = 0.07x + 0.42$ns	$y = 0.07x + 0.42$ns
TLP	$y = 0.99x - 2.21$**	$y = 1.00x - 2.24$**
Photosynthetic safety margin	$y = -1.05x + 1.82$**	$y = -1.05x + 1.82$**
Relationship to $\psi_{50} A_{max}$		
TLP	$y = 0.47x - 0.31$***	$y = 0.47x - 0.31$***

Dependent variables are P/E_p and $\psi_{50} A_{max}$ as indicated by left-justified row labels; independent variables predicted from each indicated by indented row labels. Superscripts denote the statistical significance of regressions ($P < 0.1$; **, $P < 0.01$; ***, $P < 0.001$; ns $P > 0.1$, not significant).

differences in ψ_{leaf} between pre-drought and rehydrated treatments for species *E. regnans* and *E. tricarpa* ($P_{df=36} > 0.1$, paired tests within mixed model). However, within *E. dumosa*, ψ_{leaf} of rehydrated plants was about 0.4 MPa more negative than pre-drought plants ($P_{df=36} = 0.04$).

Discussion

Collectively, our results show that sensitivity of photosynthesis to limitations within mesophyll cells varies across closely related species in an adaptive fashion, with species from drier habitats experiencing less steep declines in mesophyll photosynthetic capacity as ψ_{leaf} decreases (that is, they exhibit smaller β at more negative values of ψ_{50}; Fig 2). While changes in A_{max} with ψ_{leaf} were noisy, and we acknowledge that excluding repeated measurements from the model results in a violation of assumptions for the few plants that were repeatedly measured, the observed relations between ψ_{50} and β with P/E_p were very highly significant and considerably explanatory. Thus, we find that plants from drier climates have less mesophyll photosynthetic sensitivity to declines in ψ_{leaf}.

Ordinary and phylogenetically structured linear regressions were identical or nearly identical in these cases, suggesting almost no phylogenetic signal affecting these relationships. This lack of phylogenetic signal is somewhat surprising, and may point to an adaptive importance of MPS. However, ordinary and phylogenetically structured ANCOVAs revealed a significant difference in the intercept of the slope of βA_{max} vs P/E_p between the two subgenera (Table S3), suggesting their divergence in the rate of change in MPS across our macroclimatic gradient – and an impact of phylogeny on the results. In these cases, subgenus *Eucalyptus* had a significantly greater sensitivity for a given P/E_p
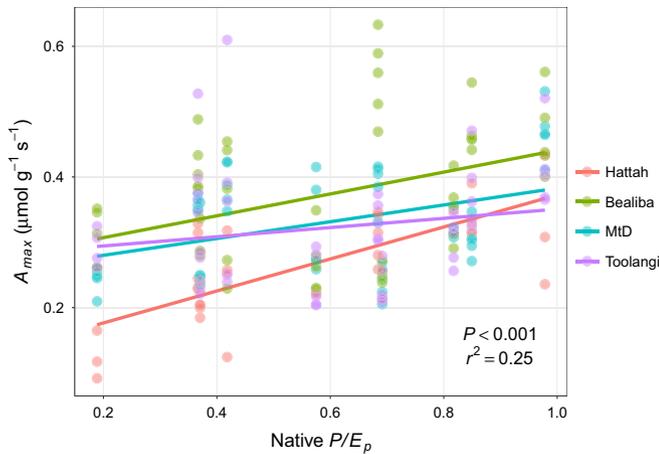
Fig. 3 $MaxA_{max}$ vs P/E_p in a common garden field experiment. Gross photosynthesis (A_{max}) was measured when water was not limiting (before drought-induced declines from mesophyll photosynthetic sensitivity) in each of four common gardens in Victoria, Australia. The (up to) five largest values were used for each species × site combination. This estimate of $MaxA_{max}$ increased with relative moisture supply of the species' native habitat. P/E_p is the ratio of annual precipitation to annual pan evaporation.

than subgenus *Symphyomyrtus*, albeit based on a small sample size. In this regard, it is interesting that the mallee and mallet habits – adapted to arid and semi-arid conditions – are far more common in subgenus *Symphyomyrtus* than subgenus *Eucalyptus* (see Thornhill *et al.*, 2019). Observed relationships of both β and ψ_{50} metrics to native moisture availability (P/E_p) suggest that less steep declines in mesophyll photosynthetic capacity that occur at more severe water stress are, as we predicted, advantageous in more arid environments. The magnitude of MPS (based on ψ_{50} and β) can be best explained by macroclimatic habitat of origin, and not by similarities in phylogenetic history, as shown by the likeness between simple linear regressions and phylogenetically structured regressions (Tables 1, S1). However, the large standard deviations of β (see Table S2) suggest that ψ_{50} may be a more reliable quantification of MPS, especially when photosynthetic drought responses are noisy.

Set against the clear advantage of reduced sensitivity as shown by species from drier climates, it is our expectation that species from wetter areas (with greater MPS) would show higher A_{max} at full hydration. In our glasshouse study, *Max* A_{max} was not significantly related to native P/E_p or ψ_{50} A_{max}. This is surprising, given that increased annual rainfall generally favors thinner leaves with faster rates of photosynthesis per unit leaf mass, due to less self-shading and internal competition for CO_2 (Givnish, 1978; Gimeno *et al.*, 2019). Victorian *Eucalyptus* spp. in general exhibit the expected increases in mass-based A_{max} with mean annual rainfall (Givnish *et al.*, 2014). We further investigated this potential trade-off in four common gardens in Victoria, Australia, and found that mass-based maximum photosynthetic rates at full hydration do increase with relative moisture supply (Fig. 3), as predicted. These studies support the expected trade-off: maximum mesophyll photosynthetic capacity at full hydration comes at the price of increased sensitivity to drops in leaf water potential.
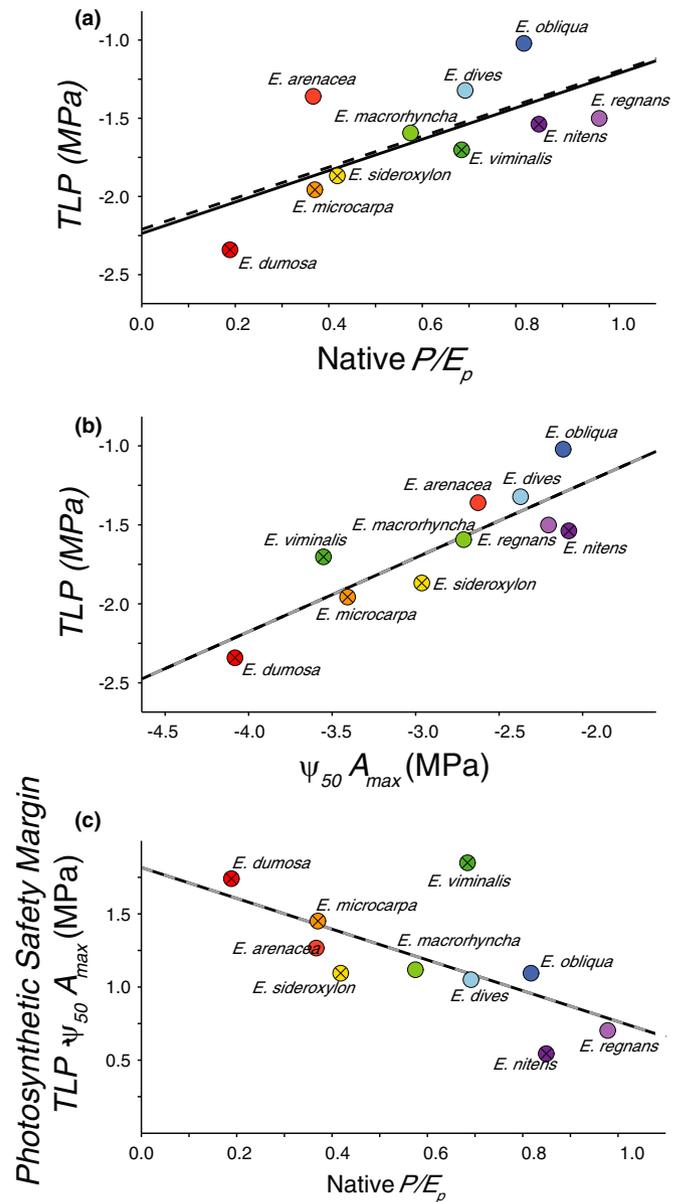
Fig. 4 Turgor loss point correlates with native P/E_p and $\psi_{50}A_{max}$. (a) Leaf water potential (ψ_{leaf}) at turgor loss (TLP) becomes less negative with increased ratio of annual precipitation to annual pan evaporation (P/E_p). (b) Species with less negative $\psi_{50}A_{max}$ (the ψ_{leaf} at a 50% decline from maximum gross photosynthetic rates) have less negative TLP. (c) Photosynthetic safety margin, the difference between TLP and $\psi_{50}A_{max}$, is smaller with increased native P/E_p. Crossed circles indicate subgenus *Symphyomyrtus*. Solid black line (a) is phylogenetically structured linear regression; dashed black line is ordinary linear regression (a); black and gray dashed lines (b,c) indicate that both types of linear regression yield the same results.

As previously predicted (Dewar *et al.*, 2018) and observed (Tezara *et al.*, 1999; Zhou *et al.*, 2013, 2014), reductions in photosynthetic carbon fixation after accounting for stomatal limitations are due to varying combinations of slower rates of carboxylation and electron transport. Reduced CO_2 conductance across the mesophyll and direct biochemical limitations can explain these declines (Tezara *et al.*, 1999; Flexas *et al.*, 2012; Dewar *et al.*, 2018). Nitrogen retranslocation and declines in
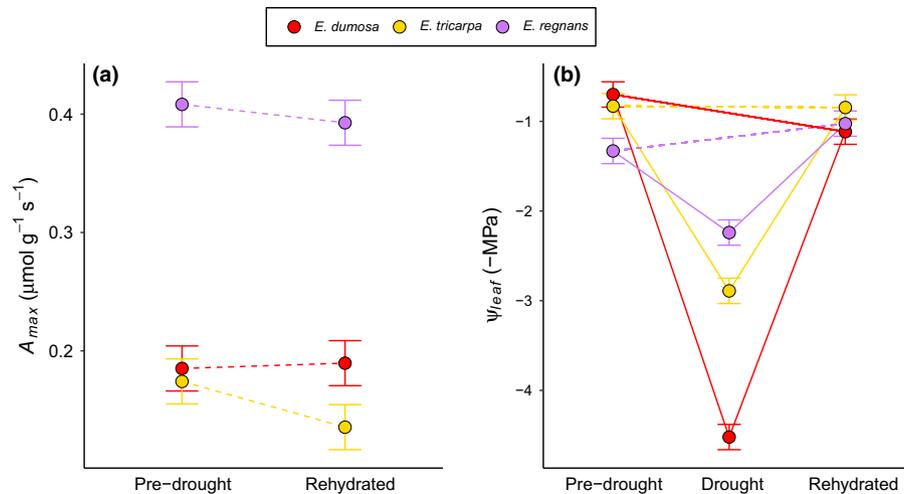
Fig. 5 Recovery of mesophyll photosynthetic capacity when plants have rehydrated after a severe drought. (a) Maximum gross photosynthetic rates (A_{max}) measured in well-hydrated plants both before drought (pre-drought) and rehydrated after experiencing a severe drought (rehydrated). Species' native habitats range from most to least arid (*Eucalyptus dumosa*, *Eucalyptus tricarpa*, *Eucalyptus regnans*, respectively) in the moisture gradient across all study species. *Eucalyptus tricarpa* is sister to *Eucalyptus sideroxylon*, which replaced the latter in this experiment. (b) Leaf water potential (ψ_{leaf}) during pre-drought, at maximum drought (drought), and during rehydrated conditions. Circles and error bars are means and SE. Dashed lines connecting two points indicate no significant difference between means ($P < 0.1$), while solid lines indicate significant difference ($P < 0.05$).

RuBisCO content might also explain these photosynthetic reductions during drought, but this effect is small (Fig. S4). While we do not tease apart the respective influences of biochemical limitation and mesophyll conductance on apparent mesophyll photosynthetic capacity in this paper, both types of nonstomatal limitations certainly contribute to observed MPS and have shown tight relationships with native soil water availability in recent studies (Zhou *et al.*, 2013, 2014).

Some assumptions within our analyses of mesophyll photosynthetic capacity and climatic distribution may have led to some error. For example, c_i values calculated during $A-c_i$ curves, which were used to estimate maximum mesophyll photosynthetic capacity, are affected by cuticular conductance and stomatal patchiness (Boyer, 2015), affecting $A-c_i$ parameterization. However, estimates of A_{max} come from what is essentially an asymptotic portion of the $A-c_i$ curve, so these small errors in c_i likely had only a small impact. In addition, while we compared ψ_{50} and β to the mean P/E_p averaged from across the distribution of each species, the seed sources did not reflect the entire range of these species. A key assumption of this study is that the between-species variation in traits or performance among taxa that occupy different, partially overlapping portions of an extensive ecological gradient will override the impact of exactly where along that gradient seeds of each taxon were chosen for propagation and study.

The tight correlation of MPS to TLP and native moisture availability reinforces the importance of MPS as a quantifiable measure of drought tolerance. Interestingly, some capacity for photosynthesis was maintained beyond wilting point; more so for species from more arid macroclimates (Fig. 4c). We interpret this as indicating that species from drier habitats have a greater safety margin between turgor loss and photosynthetic decline. Maintaining at least some capacity for photosynthesis of respired CO_2 could contribute to preventing photodamage even when leaves have wilted and stomata are closed (Bartlett *et al.*, 2016). We

acknowledge that TLPs for some species are surprisingly less negative than expected, especially considering the assimilation responses. However, the individuals measured were grown in glasshouses and were well-watered for their entire life when P–V curves were conducted. Turgor loss points have been shown to be very plastic (Bartlett *et al.*, 2014), and we suspect that the TLP values for these species may be more negative if quantified on individuals grown in their native environment and exposed to greater fluctuations in water supply. However, preliminary measurements of TLP in the common gardens taken during winter months are not very different from glasshouse results (D. D. Smith, pers. comm.).

For plants to survive beyond the end of a drought, they must be able to recover mesophyll photosynthetic capacity. We found that species from across a macroclimatic moisture gradient, and with different MPS, are all able to recover mesophyll photosynthetic rates to pre-drought capacities after substantial rehydration (Fig. 5). It must be noted that, while all three species recovered their full photosynthetic capacity, the species from the most arid habitat – with the lowest MPS – did not recover ψ_{leaf} to pre-drought conditions. We speculate that this may be caused by increases in osmolyte content during drought, allowing greater plasticity in TLP and persist after rehydration (Bartlett *et al.*, 2014). More experiments are needed to tease apart differences in recovery abilities among species, and their relationship to the duration and intensity of drought, in order to determine the extent to which MPS can be characterized as a reversible process that can be fully described by the logistic declines in A_{max} vs ψ_{leaf}, or instead as a process which involves irreversible changes.

Many studies have investigated plant gas exchange responses to drought, but few have compared mesophyll photosynthetic sensitivity among species from habitats of differing moisture supply, and to our knowledge none have accounted for phylogeny. This paper is the first phylogenetically structured, comparative analysis

of MPS across a large set of closely related species. Our findings provide important insights into a previously unexplored dimension of plant adaptive evolution to drought. We showed that species from moister habitats had greater MPS, based on ψ_{50} and β for A_{max}. A previous study qualitatively compared MPS among species from different habitats and found similar results (Zhou *et al.*, 2014), but without incorporating phylogenetically structured analyses. That study also included species with evergreen, summergreen deciduous, and wintergreen foliage, as well as species with and without N-fixing symbioses, and two species that have natural distributions set by water-table depth rather than rainfall – all of which can confound relationships between MPS and P/E_p. By showing similar quantitative relationships of various measures of MPS to native P/E_p in upland *Eucalyptus* species and incorporating phylogenetic relationships, as well as finding that MPS is tightly correlated with turgor loss point, we add significantly to our understanding of how photochemical limitations are coupled to aspects of leaf hydraulics, including stomatal and leaf hydraulic conductances (Brodribb *et al.*, 2007; Meinzer *et al.*, 2017), and our findings highlight the importance of MPS in predicting large-scale consequences of drought (see also Zhou *et al.*, 2019).

Drought limitation of photosynthesis may be greatly underestimated if its effects on nonstomatal limitations are not taken into account (Givnish, 1986; Tezara *et al.*, 1999, 2003; Lawlor & Tezara, 2009; Dewar *et al.*, 2018; Zhou *et al.*, 2019), which has important implications for plant evolution. Given that the highly diverse genus *Eucalyptus* (> 700 spp.) radiated during periods of rapid aridification from the Oligocene to the Middle Miocene (Thornhill *et al.*, 2019), selection for reduced MPS in drier habitats may have been intense at that time. According to this testable hypothesis, we would expect to see high MPS in early divergent eucalypt lines that today are restricted to especially mesic habitats (e.g. *Stockwellia* in Queensland rain forests).

Our findings on MPS provide a key missing component for our understanding of the optimization of stomatal conductance which the widely cited Cowan & Farquhar (1977) model does not take into account. When subsequent models included MPS, they reproduced the principal conclusions of the Cowan & Farquhar model (e.g. the linear relationship between photosynthetic rate and stomatal conductance across time and space) in a more quantitative fashion (Givnish, 1986; Dewar *et al.*, 2018). Our findings have important implications for the evolution of stomatal conductance, which in turn has cascading potential impacts on large-scale patterns in transpiration, productivity, and climate (Webb *et al.*, 1983; Boyce *et al.*, 2009; Medlyn *et al.*, 2011; Zhou *et al.*, 2019). More broadly, MPS likely played a central role in plants' transition to life on land. Studies of MPS on kelp (which, like the first terrestrial plants, lack stomata) confirm that photosynthesis slows dramatically as leaf water potential becomes more negative (Kawamitsu *et al.*, 2000; Berry *et al.*, 2010; Chater *et al.*, 2017). The first land plants would have greatly benefited from adaptations including not only root allocation, vascular systems, and stomata as previously hypothesized (Givnish, 1986; Berry *et al.*, 2010), but also reduced sensitivity of mesophyll photosynthetic capacity to leaf water potential.

Author contributions

The project was conceived and designed by TJG, KAM and AMS. AMS, DDS and MAA carried out measurements. AMS analyzed data with assistance from DDS, KAM and TJG. AMS, TJG and KAM wrote the manuscript with help from DDS and MAA.

ORCID

Mark A. Adams https://orcid.org/0000-0002-8154-0097
Thomas J. Givnish https://orcid.org/0000-0003-3166-4566
Katherine A. McCulloh https://orcid.org/0000-0003-0801-3968
Amanda M. Salvi https://orcid.org/0000-0001-7230-4167
Duncan D. Smith https://orcid.org/0000-0002-7294-3812

Data availability

The data supporting the results are available as Supporting Information files and via the Dryad depository: doi: 10.5061/dryad.rn8pk0p8v.

References

Ball MC, Farquhar GD. 1984. Photosynthetic and stomatal responses of two mangrove species, *Aegiceras corniculatum* and *Avicennia marina*, to long term salinity and humidity conditions. *Plant Physiology* 74: 1–6.

Bartlett MK, Klein T, Jansen S, Choat B, Sack L. 2016. The correlations and sequence of plant stomatal, hydraulic, and wilting responses to drought. *Proceedings of the National Academy of Sciences, USA* 113: 13098–13103.

Bartlett MK, Scoffoni C, Sack L. 2012. The determinants of leaf turgor loss point and prediction of drought tolerance of species and biomes: a global meta-analysis. *Ecology Letters* 15: 393–405.

Bartlett MK, Zhang Y, Kreidler N, Sun S, Ardy R, Cao K, Sack L. 2014. Global analysis of plasticity in turgor loss point, a key drought tolerance trait. *Ecology Letters* 17: 1580–1590.

Berry JA, Beerling DJ, Franks PJ. 2010. Stomata: Key players in the earth system, past and present. *Current Opinion in Plant Biology* 13: 232–239.

Boyce CK, Brodribb TJ, Feild TS, Zwieniecki MA. 2009. Angiosperm leaf vein evolution was physiologically and environmentally transformative. *Proceedings of the Royal Society: Biological Sciences* 276: 1771–1776.

Boyer JS. 2015. Impact of cuticle on calculations of the CO_2 concentration inside leaves. *Planta* 242: 1405–1412.

Brodribb TJ, Feild TS, Jordan GJ. 2007. Leaf maximum photosynthetic rate and venation are linked by hydraulics. *Plant Physiology* 144: 1890–1898.

Bui EN, Thornhill AH, González-Orozco CE, Knerr N, Miller JT. 2017. Climate and geochemistry as drivers of eucalypt diversification in Australia. *Geobiology* 15: 427–440.

Carriquí M, Cabrera HM, Conesa M, Coopman RE, Douthe C, Gago J, Gallé A, Galmés J, Ribas-Carbo M, Tomás M *et al.* 2015. Diffusional limitations explain the lower photosynthetic capacity of ferns as compared with angiosperms in a common garden study. *Plant, Cell & Environment* 38: 448–460.

Cernusak LA, Hutley LB, Beringer J, Holtum JAM, Turner BL. 2011. Photosynthetic physiology of eucalypts along a sub-continental rainfall gradient in northern Australia. *Agricultural and Forest Meteorology* 151: 1462–1470.

Chater CCC, Caine RS, Fleming AJ, Gray JE. 2017. Origins and evolution of stomatal development. *Plant Physiology* 174: 624–638.

Cowan IR, Farquhar GD. 1977. Stomatal function in relation to leaf metabolism and environment. *Symposia of the Society for Experimental Biology* 31: 471–505.

Crisp M, Cook L, Steane D. 2004. Radiation of the Australian flora: what can comparisons of molecular phylogenies across multiple taxa tell us about the evolution of diversity in present-day communities? *Philosophical Transactions of the Royal Society B: Biological Sciences* 359: 1551–1571.

Dewar R, Mauranen A, Mäkelä A, Hölttä T, Medlyn BE, Vesala T. 2018. New insights into the covariation of stomatal, mesophyll and hydraulic conductances from optimization models incorporating nonstomatal limitations to photosynthesis. *New Phytologist* 217: 571–585.

Duursma RA. 2015. Plantecophys - An R package for analysing and modelling leaf gas exchange data. *PLoS ONE* 10: 1–13.

Farquhar GD, von Caemmerer S, Berry JA. 1980. A biochemical model of photosynthetic CO_2 assimilation in leaves of C3 species. *Planta* 149: 78–90.

Fick SE, Hijmans RJ. 2017. WorldClim 2: new 1-km spatial resolution climate surfaces for global land areas. *International Journal of Climatology* 37: 4302–4315.

Flexas J, Barbour MM, Brendel O, Cabrera HM, Carriquí M, Díaz-Espejo A, Douthe C, Dreyer E, Ferrio JP, Gago J *et al.* 2012. Mesophyll diffusion conductance to CO_2: an unappreciated central player in photosynthesis. *Plant Science* 193–194: 70–84.

Flexas J, Carriquí M, Nadal M. 2018. Gas exchange and hydraulics during drought in crops: Who drives whom? *Journal of Experimental Botany* 69: 3791–3795.

Flexas J, Díaz-Espejo A, Berry JA, Cifre J, Galmés J, Kaldenhoff R, Medrano H, Ribas-Carbó M. 2007. Analysis of leakage in IRGA's leaf chambers of open gas exchange systems: quantification and its effects in photosynthesis parameterization. *Journal of Experimental Botany* 58: 1533–1543.

Fu X, Meinzer FC. 2018. Metrics and proxies for stringency of regulation of plant water status (iso/anisohydry): a global data set reveals coordination and trade-offs among water transport traits. *Tree Physiology* 39: 122–134.

Gago J, Carriquí M, Nadal M, Clemente-Moreno MJ, Coopman RE, Fernie AR, Flexas J. 2019. Photosynthesis optimized across land plant phylogeny. *Trends in Plant Science* 24: 947–958.

Galmés J, Aranjuelo I, Medrano H, Flexas J. 2013. Variation in Rubisco content and activity under variable climatic factors. *Photosynthesis Research* 117: 73–90.

Gimeno TE, Saavedra N, Ogée J, Medlyn BE, Wingate L. 2019. A novel optimization approach incorporating non-stomatal limitations predicts stomatal behaviour in species from six plant functional types. *Journal of Experimental Botany* 70: 1639–1651.

Givnish TJ. 1978. Ecological aspects of plant morphology: leaf form in relation to environment. *Acta Biotheoretica* 27: 83–142.

Givnish TJ. 1986. Optimal stomatal conductance, allocation of energy between leaves and roots, and the marginal cost of transpiration. In: Givnish TJ, ed. *On the economy of plant form and function*. Cambridge, UK: Cambridge University Press, 171–213.

Givnish TJ. 1988. Adaptation to sun and shade: a whole-plant perspective. *Australian Journal of Plant Physiology* 15: 63–92.

Givnish TJ, Montgomery RA. 2014. Common-garden studies on adaptive radiation of photosynthetic physiology among Hawaiian lobeliads. *Proceedings of the Royal Society B: Biological Sciences* 281: 20132944.

Givnish TJ, Vermeij G. 1976. Sizes and shapes of liane leaves. *American Naturalist* 110: 743–778.

Givnish TJ, Wong SC, Stuart-Williams H, Holloway-Phillips M, Farquhar GD. 2014. Determinants of maximum tree height in *Eucalyptus* species along a rainfall gradient in Victoria, Australia. *Ecology* 95: 2991–3007.

Grassi G, Magnani F. 2005. Stomatal, mesophyll conductance and biochemical limitations to photosynthesis as affected by drought and leaf ontogeny in ash and oak trees. *Plant, Cell & Environment* 28: 834–849.

Ho LST, Ané C. 2014. A linear-time algorithm for gaussian and non-gaussian trait evolution models. *Systematic Biology* 63: 397–408.

Kawamitsu Y, Driscoll T, Boyer JS. 2000. Photosynthesis during desiccation in an intertidal alga and a land plant. *Plant and Cell Physiology* 41: 344–353.

Knauer J, Zaehle S, De Kauwe MG, Haverd V, Reichstein M, Sun Y. 2020. Mesophyll conductance in land surface models: effects on photosynthesis and transpiration. *The Plant Journal* 101: 858–873.

Kruger EL, Volin JC. 2006. Reexamining the empirical relation between plant growth and leaf photosynthesis. *Functional Plant Biology* 33: 421–429.

Lawlor DW, Tezara W. 2009. Causes of decreased photosynthetic rate and metabolic capacity in water-deficient leaf cells: a critical evaluation of mechanisms and integration of processes. *Annals of Botany* 103: 561–579.

Li X, Blackman CJ, Choat B, Duursma RA, Rymer PD, Medlyn BE, Tissue DT. 2018. Tree hydraulic traits are coordinated and strongly linked to climate-of-origin across a rainfall gradient. *Plant, Cell & Environment* 41: 646–660.

Medlyn BE, Duursma RA, Eamus D, Ellsworth DS, Prentice IC, Barton CVM, Crous KY, De Angelis P, Freeman M, Wingate L. 2011. Reconciling the optimal and empirical approaches to modelling stomatal conductance. *Global Change Biology* 17: 2134–2144.

Meinzer FC, Smith DD, Woodruff DR, Marias DE, McCulloh KA, Howard AR, Magedman AL. 2017. Stomatal kinetics and photosynthetic gas exchange along a continuum of isohydric to anisohydric regulation of plant water status. *Plant, Cell & Enviornment* 40: 1618–1628.

Miller JM, Williams RJ, Farquhar GD. 2001. Carbon isotope discrimination by a sequence of *Eucalyptus* species along a subcontinental rainfall gradient in Australia. *Functional Ecology* 15: 222–232.

Nadal M, Flexas J. 2018. Mesophyll conductance to CO_2 diffusion: effects of drought and opportunities for improvement. In: García-Tejero IF, Durán-Zuazo VH, eds. *Water scarcity and sustainable agriculture in semiarid environment*. London, UK: Elsevier, 403–438.

Nicolle D. 2006. Eucalypts of Victoria and Tasmania. Melbourne, Vic., Australia: Bloomings Books.

Orians GH, Solbrig OT. 1977. A cost-income model of leaves and roots with species reference to arid and semiarid areas. *American Naturalist* 111: 677–690.

QGIS Development Team. 2018. *QGIS geographic information system.* [WWW document} URL https://www.osgeo.org/. Open Source Geospatial Foundation Project.

R Core Team. 2019. *R: a language and environment for statistical computing. R v. 3.6.2.* Vienna, Austria: R Foundation for Statistical Computing. [WWW document] URL https://www.R-project.org/ [accessed 17 March 2021].

Revell LJ. 2012. phytools: an R package for phylogenetic comparative biology (and other things). *Methods in Ecology and Evolution* 3: 217–223.

Salmon Y, Lintunen A, Dayet A, Chan T, Dewar R, Vesala T, Hölttä T. 2020. Leaf carbon and water status control stomatal and nonstomatal limitations of photosynthesis in trees. *New Phytologist* 226: 690–703.

Schulze ED, Turner NC, Nicolle D, Schumacher J. 2006. Leaf and wood carbon isotope ratios, specific leaf areas and wood growth of *Eucalyptus* species across a rainfall gradient in Australia. *Tree Physiology* 26: 479–492.

Schulze ED, Williams RJ, Farquhar GD, Schulze W, Langridge J, Miller JM, Walker BH. 1998. Carbon and nitrogen isotope discrimination and nitrogen nutrition of trees along a rainfall gradient in northern Australia. *Australian Journal of Plant Physiology* 25: 413–425.

Tang AC, Kawamitsu Y, Kanechi M, Boyer JS. 2002. Photosynthetic oxygen evolution at low water potential in leaf discs lacking an epidermis. *Annals of Botany* 89: 861–870.

Temme AA, Kerr KL, Donovan LA. 2019. Vigour/tolerance trade-off in cultivated sunflower (*Helianthus annuus*) response to salinity stress is linked to

leaf elemental composition. *Journal of Agronomy and Crop Science* **205**: 508–518.

Tezara W, Martínez D, Rengifo E, Herrera A. 2003. Photosynthetic responses of the tropical spiny shrub *Lycium nodosum* (*Solanaceae*) to drought, soil salinity and saline spray. *Annals of Botany* **92**: 757–765.

Tezara W, Mitchell VJ, Driscoll SD, Lawlor DW. 1999. Water stress inhibits plant photosynthesis by decreasing coupling factor and ATP. *Nature* **401**: 914–917.

Tezara W, Mitchell V, Driscoll SD, Lawlor DW. 2002. Effects of water deficit and its interaction with CO_2 supply on the biochemistry and physiology of photosynthesis in sunflower. *Journal of Experimental Botany* **53**: 1781–1791.

Thornhill AH, Crisp MD, Külheim C, Lam KE, Nelson LA, Yeates DK, Miller JT. 2019. A dated molecular perspective of eucalypt taxonomy, evolution, and diversification. *Australian Systematic Botany* **32**: 29–48.

Turner NC, Schulze ED, Nicolle D, Schumacher J, Kuhlmann I. 2008. Annual rainfall does not directly determine the carbon isotope ratio of leaves of *Eucalyptus* species. *Physiologia Plantarum* **132**: 440–445.

Tyree MT, Hammel HT. 1972. The measurement of the turgor pressure and the water relations of plants by the pressure-bomb technique. *Journal of Experimental Botany* **23**: 267–282.

Wang X, Du T, Huang J, Peng S, Xiong D. 2018. Leaf hydraulic vulnerability triggers the decline in stomatal and mesophyll conductance during drought in rice. *Journal of Experimental Botany* **69**: 4033–4045.

Warren CR, Adams MA. 2005. What determines interspecific variation in relative growth rate of *Eucalyptus* seedlings? *Oecologia* **144**: 373–381.

Warren CR, Dreyer E, Tausz M, Adams MA. 2006. Ecotype adaptation and acclimation of leaf traits to rainfall in 29 species of 16-year-old *Eucalyptus* at two common gardens. *Functional Ecology* **20**: 929–940.

Webb WL, Lauenroth WK, Szarek SR, Kinerson RS. 1983. Primary production and abiotic controls in forests, grasslands, and desert ecosystems in the United States. *Ecology* **64**: 134–151.

Wickham H. 2016. *ggplot2: Elegant Graphics for Data Analysis.* New York, NY, USA: Springer-Verlag.

Xiong D, Douthe C, Flexas J. 2018. Differential coordination of stomatal conductance, mesophyll conductance, and leaf hydraulic conductance in response to changing light across species. *Plant, Cell & Environment* **41**: 436–450.

Zhou S, Duursma RA, Medlyn BE, Kelly JWG, Prentice IC. 2013. How should we model plant responses to drought? An analysis of stomatal and non-stomatal responses to water stress. *Agricultural and Forest Meteorology* **182**: 204–214.

Zhou S, Medlyn BE, Sabaté S, Sperlich D, Prentice IC. 2014. Short-term water stress impacts on stomatal, mesophyll and biochemical limitations to photosynthesis differ consistently among tree species from contrasting climates. *Tree Physiology* **34**: 1035–1046.

Zhou SX, Prentice IC, Medlyn BE. 2019. Bridging drought experiment and modeling: Representing the differential sensitivities of leaf gas exchange to drought. *Frontiers in Plant Science* **9**: 1–12.

Supporting Information

Additional Supporting Information may be found online in the Supporting Information section at the end of the article.

Fig. S1 Molecular phylogeny of the 10 *Eucalyptus* species.

Fig. S2 Raw data for sensitivity of maximum gross photosynthetic rate (A_{max}) to leaf water potential (ψ_{leaf}).

Fig. S3 Model selection for A_{max} vs ψ_{leaf}.

Fig. S4 Box-plot diagram of percent leaf nitrogen content before and after drought experiments.

Fig. S5 Shifts in sensitivity of apparent V_{cmax} and J_{max} to leaf water potential.

Fig. S6 Raw data for sensitivity of apparent maximum carboxylation rate (V_{cmax}) to leaf water potential.

Fig. S7 Raw data for sensitivity of apparent maximum electron transport rate (J_{max}) to leaf water potential.

Table S1 Mesophyll photosynthetic sensitivity trait values and estimated errors of the 10 *Eucalyptus* species.

Table S2 Geographic coordinates, climatic and soil information for the four common gardens in Victoria, Australia.

Table S3 Statistical results of linear regressions.

Please note: Wiley Blackwell are not responsible for the content or functionality of any Supporting Information supplied by the authors. Any queries (other than missing material) should be directed to the *New Phytologist* Central Office.